

COLD H<sub>2</sub>O AND CO ICE AND GAS TOWARD THE GALACTIC CENTER<sup>1</sup>

ANDREA MONETI

CSIC, IEM, Dpto. Física Molecular, Serrano 121, E-28006 Madrid, Spain.  
e-mail: amoneti@astro.iem.csic.es

JOSÉ CERNICHARO

CSIC, IEM, Dpto. Física Molecular, Serrano 121, E-28006 Madrid, Spain.  
Division of Physics, Mathematics and Astronomy, California Institute of Technology,  
MS 320-47, Pasadena, CA 91125, USA  
e-mail: cerni@astro.iem.csic.es

JUAN RAMÓN PARDO

Division of Physics, Mathematics and Astronomy, California Institute of Technology,  
MS 320-47, Pasadena, CA 91125, USA  
e-mail: pardo@submm.caltech.edu

## ABSTRACT

We present observations of CO, <sup>13</sup>CO and of H<sub>2</sub>O in the middle and far-infrared taken with the ISO-SWS and ISO-LWS spectrometers toward two positions in the Galactic Center region (Sgr A\* and GCS-3). Both ice and gas phase molecules are detected. The ISO data have been complemented with observations of the J=3-2 and J=7-6 lines of CO carried out at the Caltech Submillimeter Observatory. The ISO and CSO data indicate that the absorbing gas is extremely cold,  $T_K \simeq 10$  K, suggesting that it is located in the dark clouds of the different spiral arms that intersect the line of sight towards the Galactic Center. From the analysis of the CO absorption we derive <sup>13</sup>CO gas phase column densities of 1.1 and 0.7 10<sup>17</sup> cm<sup>-2</sup> towards Sgr A\* and GCS-3 respectively. The H<sub>2</sub>O gas column density in the direction of Sgr A\* is  $\simeq 2 \cdot 10^{16}$  cm<sup>-2</sup>. The derived CO/H<sub>2</sub>O and gas/solid abundance ratios corresponding to these cold clouds are remarkably similar along the two lines of sight. We find that nearly all the CO is in the gas phase, while the H<sub>2</sub>O is almost entirely frozen onto the surfaces of cold dust grains. Finally, the  $N_{gas+ice}(CO)/N_{gas+ice}(H_2O)$  abundance ratio is  $\simeq 5$  implying that H<sub>2</sub>O formation processes are highly efficient.

*Subject headings:* ISM: molecules, abundances, individual (Sgr A\*, GCS-3) — Infrared : ISM lines and bands

## 1. INTRODUCTION

The water molecule plays an important role in the chemistry of interstellar and circumstellar clouds. However, due to its high abundance in the terrestrial atmosphere, its rotational, vibrational, and electronic transitions of the main isotopic species are mostly hidden from view from ground-based telescopes (except for some weak rotational lines, see Cernicharo et al. 1990, 1994). It was only with the advent of the Infrared Space Observatory (ISO, Kessler et al., 1999) that extensive observations of the far-infrared thermal lines of water vapor could be used to obtain reliable estimates of the water vapor abundance in molecular clouds. Mapping of the Sgr B2 molecular cloud with ISO by Cernicharo et al. (1997a) has definitely shown that H<sub>2</sub>O is a ubiquitous molecule in the cores of warm molecular clouds with an abundance of  $\simeq 10^{-5}$ . In addition, maps of the emission of several H<sub>2</sub>O lines in Orion IRC2 have been obtained by Cernicharo et al. (1997b, 1999) showing that the abundance of H<sub>2</sub>O is close to 10<sup>-4</sup> in the shocked gas. H<sub>2</sub>O observations of the central position of Orion have been also obtained by van Dishoeck et al. (1998), González-Alfonso et al. (1998) and Harwit et al. (1998). All these new data refer to the warm regions of molecular clouds. While there is also strong evidence for a high water depletion onto the ice mantles of dust grains

in the coldest regions, no water vapor has been detected in the direction of dark clouds, probably due to the low temperature and density prevailing in these objects.

In order to study the coldest and least disturbed regions of molecular clouds, we have examined the ISO archive spectra of two positions in the Galactic Center, where absorption from the intervening medium is known to occur (Geballe, Baas, and Wade 1989, Lutz et al. 1996, Okuda et al. 1990). In the case of Sgr A\*, this cold gas is also seen in the form of sharp and deep absorption features at 0, -30, and -50 km s<sup>-1</sup> in various millimeter transitions of NH<sub>3</sub> and CO against the broad background produced by the warm clouds in Sgr A West (Serabyn and Güsten 1986, Sutton et al. 1990). These data, together with submillimeter observations of the J=3-2 and J=7-6 lines of CO, have been modeled to place constraints on the abundances of these molecules in both the gas and the solid phase.

## 2. OBSERVATIONS

All data were obtained with the ISO Short and Long Wavelength Spectrometers (SWS, de Graauw et al. 1999; LWS, Clegg et al., 1999) using the full resolution grating mode of the SWS ( $\lambda/\Delta\lambda \simeq 1500$ –2000) and the grating

<sup>1</sup>Based on observations with ISO, an ESA project with instruments funded by ESA Member States (especially the PI countries: France Germany, the Netherlands and the United Kingdom) and with the participation of ISAS and NASA.

and Fabry Perot (FP) modes of the LWS ( $\lambda/\Delta\lambda \simeq 300$  and 9000 respectively). The effective SWS aperture in the 4–7  $\mu\text{m}$  range is about  $14'' \times 20''$ , while the LWS aperture is circular and  $\sim 70''$  in diameter. In the case of GCS-3, the aperture was centered on GCS-3 I, though the brightest source in the aperture at 5  $\mu\text{m}$  is GCS-3 II (Moneti et al. 1999). The aperture centered on Sgr A\* also includes several point-like and diffuse sources. OLP 7.1 archive data were further processed with the ISAP package<sup>1</sup>. The results are shown in Figures 1, 2 and 3. In order to resolve the velocity structure of the absorbing/emitting gas in the direction of Sgr A\* we have made observations of the J=3-2 and J=7-6 lines of CO in the direction of this source with the CSO telescope. These observations were made in position switching, with the off position 4 degrees outside the galactic plane. A region of 10x6 arcminutes was mapped in the J=3-2 line of CO and a few positions were observed in the J=7-6 line of the same species. The system temperatures at the frequencies of the J=3-2 and J=7-6 lines of CO were 760 and 6000 K respectively and the spectral resolution was 0.5 MHz. The results for the central position of our maps, Sgr A\*, are shown in Figure 3.

### 3. RESULTS AND DISCUSSION

In order to determine the physical conditions of the foreground cold gas from the ISO H<sub>2</sub>O and CO data, we have used an ETL model with line parameters from the HITRAN molecular database (Rothman et al., 1993) to find the best fit to the line absorption. We note, however, that the energies of all ortho levels of H<sub>2</sub>O are referred in HITRAN to the ground state of para-H<sub>2</sub>O, i.e., the energy of the 1<sub>01</sub> ground state of ortho-H<sub>2</sub>O is not set equal to zero. For very low rotational temperatures the derived physical parameters will have a large error if the HITRAN values of the energies and line intensities (which include a Boltzmann factor) are not corrected.

The J=7-6 line of CO shows emission over a broad velocity range (see Figure 3). The shape of this broad emission changes smoothly with position. This gas is certainly warm and emits in high-J lines of CO as shown in the LWS grating data of Sgr A\* (see inset panel in Figure 3b). The J=3-2 line shows several narrow features in absorption against the broad component arising in the vicinity of Sgr A\*. These narrow absorptions (see Figure 3), at velocities of 0, -30 and -50 km<sup>-1</sup> have been also seen in many other molecular and atomic species, and do correspond to cold gas in the line of sight which produces the series of R and P lines up to J=7 in the ro-vibrational band of CO (see Figure 1). Mapping with the CSO of both CO lines indicates that the absorption features are present in all positions where the broad emission is seen. These absorptions appear in all observed positions (10x6 arcminutes). Hence, both broad emission and narrow lines fill the ISO LWS and SWS beams. Consequently, prior to the analysis of the ro-vibrational absorption, the broad components due to the ices and, in the case of Sgr A\* to the warm CO gas in the Sgr A West region (Sutton et al. 1990), had to be analyzed and removed. In the following discussion we will assume  $x(\text{CO}) = 10^{-4}$  and  $^{12}\text{CO}/^{13}\text{CO} = 60$  (Langer

and Wilson 1990).

#### 3.1. Modeling the Warm CO Gas in Sgr A West

This warm component is clearly visible in Figure 1 and 3 (high-J CO lines; inset panel in Figure 3b). The CO ro-vibrational data (SWS) have been modeled by a single component with  $T_{\text{rot}} = 150$  K,  $\Delta v = 200$  km s<sup>-1</sup>, and  $N(\text{CO}) = 1.0 \cdot 10^{17}$  cm<sup>-2</sup>. The assumed linewidth is suggested by our J=7-6 line data and by the LWS Fabry Perot (LWS-FP) observations of some CO lines (not shown here). The LWS-grating data toward Sgr A\* show CO pure rotational line emission from the  $J = 14$ –13 up to the  $J = 21$ –20 transitions (some of them are shown in the inset panel of Figure 3b). Assuming that the emission fills the beam, and using a large velocity gradient code and the collisional rates of Schinke et al. (1985), the observed intensities are reproduced, within 20–30%, for  $n(\text{H}_2) = 3 \cdot 10^5$  cm<sup>-3</sup>,  $T_K = 250$  K,  $N(\text{CO}) = 1.2 \cdot 10^{17}$  cm<sup>-2</sup> with the assumed linewidth. The corresponding excitation temperatures vary between 160 to 180 K from the  $J = 14$ –13 to the  $J = 21$ –20 rotational lines of CO, i.e., similar to the rotation temperature derived from the SWS ro-vibrational absorption of CO. Note that the region is rather complex and that the column density we derive represents a beam averaged value. Column densities for individual clouds could be larger and have to be derived using the corresponding filling factor and the correct linewidths. The values for  $n(\text{H}_2)$  and  $T_K$  are in excellent agreement with those derived by Sutton et al. (1990) for the individual warm clouds. The region of GCS-3 is free of molecular emission (Serabyn and Güsten 1991), and thus no such warm gas was used in the GCS-3 model.

#### 3.2. The CO and H<sub>2</sub>O ices

The CO, XCN, and H<sub>2</sub>O ices shown in our spectra are among those that are commonly found in the direction of young sources deeply embedded in molecular clouds. The CO and XCN ice absorption bands were modeled as simple Gaussians; two Gaussians of different widths and central wavelengths were used for the polar and non-polar CO ices (Chiar et al. 1998). The main goal of this fitting was to remove the CO-ice contribution from the continuum, nevertheless we could derive  $N(\text{CO-ice}) \simeq 1.4 \cdot 10^{17}$  and  $\simeq 0.7 \cdot 10^{17}$  cm<sup>-2</sup> for Sgr A\* and GCS-3, respectively, with  $\sim 70\%$  apolar in Sgr A\*, and  $\sim 45\%$  apolar in GCS-3. Our value of  $N(\text{CO-ice})$  in Sgr A\* is twice that derived by McFadzean et al. (1989) from lower resolution spectroscopy. As for the H<sub>2</sub>O ice, Chiar et al. (2000) used the same SWS data discussed here, but considered both the 6  $\mu\text{m}$  and the 3  $\mu\text{m}$  water ice features to determine  $N(\text{H}_2\text{O-ice}) \simeq 1.2 \cdot 10^{18}$  cm<sup>-2</sup> and  $5 \cdot 10^{17}$  cm<sup>-2</sup> for Sgr A\* and GCS-3, respectively.

The high fraction of apolar CO-ice and the high  $N(\text{CO})/N(\text{H}_2\text{O})$  ratios, together with the deep absorption of CO<sub>2</sub> ice (Whittet et al. 1997), are typical of cold, quiescent environments (Chiar et al. 1998), indicating that these ices cannot be located in the warm clouds in Sgr A West.

<sup>1</sup>ISAP is a joint development of the LWS and SWS instrument teams and data cent-res. Contributing institutes are CNRS, IAS, IPAC, MPE, RAL, and SRON.

### 3.3. The cold CO gas

Due to the heavy saturation of the  $^{12}\text{CO}$  ro-vibrational lines (opacities of about 20–30), the physical parameters of the cold CO gas were determined from the  $^{13}\text{CO}$  and the adopted isotopic abundance ratio. Three components at the velocities indicated by the J=3-2 absorption features in Figure 3 were used in the model, with linewidths  $\Delta v = 12 \text{ km s}^{-1}$  as measured in our data. These linewidths agree well with the results shown in Figure 1 of Sutton et al. (1990). The derived model parameters (column density and rotation temperature) are the same for the three components. Model results can be found in Table 1. A single  $\text{C}^{18}\text{O}$  velocity component was introduced in order to fit the weak  $R(0)$  line of this isotope. We also find that in both lines of sight the cold gas alone is not sufficient to reproduce completely the  $^{12}\text{CO}$  absorption, and a component of higher kinetic temperature,  $T \simeq 40 \text{ K}$ , and  $N \simeq 1\%$  of the total, is necessary to account for the highest observed  $J$  lines. This component cannot arise from an incomplete removal of the warm gas in Sgr A West, since it is present in both spectra, and should correspond to dense cloud material ( $n(\text{H}_2) > 5 \cdot 10^4 \text{ cm}^{-3}$ ) of low CO column density. We estimate uncertainties of about a factor of 2 in the column densities. The volume density needed to pump the observed rotational levels of the CO ground state is around  $3 \cdot 10^4 \text{ cm}^{-3}$  in the case of  $T_{\text{rot}} \simeq 10 \text{ K}$  (Sgr A\*), decreasing to  $\simeq 1000 \text{ cm}^{-3}$  at  $\simeq 5 \text{ K}$  (GSC-3). Adopting  $A_V/N(\text{H}_2) \simeq 2 \cdot 10^{-21} \text{ mag/cm}^{-2}$ , the cold CO column densities imply visual extinction of 33 and 21 mag towards Sgr A\* and GCS-3, respectively, generally consistent with values in the literature.

### 3.4. The cold/warm $\text{H}_2\text{O}$ gas

In contrast to CO, the  $\text{H}_2\text{O}$  absorption at  $6 \mu\text{m}$  is weak: 3% ( $8\sigma$ ) in Sgr A\*, and 2% ( $3\sigma$ ) in GCS-3 (not shown). The three features detected are the  $0_{00}-1_{11}$  (para), and the  $1_{01}-1_{10}$  and  $1_{01}-2_{12}$  (ortho) lines of the  $\nu_2 = 0 \rightarrow 1$  vibrational transition of water vapor (see Figure 1f). In the Sgr A\* data, the para transition is blended with the  $\text{H}_2$  (0,0) S(6) line, which was removed by assuming an intensity of  $1/3$  the average of the S(5) and S(7) lines. The para line of  $\text{H}_2\text{O}$  is present before the subtraction of the S(6) line of  $\text{H}_2$ , however, its intensity is poorly determined. Features B & C in Figure 1f are ortho- $\text{H}_2\text{O}$  while A corresponds to para- $\text{H}_2\text{O}$ . Figure 1g shows the  $\text{H}_2\text{O}$  levels involved in these transitions. All three absorption features arise from the ground para and ortho states to the first excited rotational levels of the bending mode of water vapor. The lack of other  $\text{H}_2\text{O}$  absorption features indicates that all the water molecules are in the ground state (ortho and para). An ortho/para abundance ratio of 3 has been assumed.

The best fit to the  $\text{H}_2\text{O}$  absorption, assuming also the three velocity components of CO, is obtained for  $T_{\text{rot}} \simeq 8 \text{ K}$ , similar to the temperatures deduced from CO. While these  $\text{H}_2\text{O}$  lines are not very sensitive to temperature in the 3–12 K range, an upper limit  $T_{\text{rot}} \lesssim 12 \text{ K}$  is obtained from the lack of absorption from the  $1_{10}$  ortho level which is 26.7 K above the ortho ground state (absorption from other levels of para water is more difficult as the first excited level, the  $1_{11}$ , is 53.4 K above the para ground state). The ro-vibrational line opacities are  $\simeq 1$  and  $\simeq 0.3$  for the

ortho and para species, respectively. The column density of  $\text{H}_2\text{O}$  is  $2 \cdot 10^{16} \text{ cm}^{-2}$  with little dependence on the assumed  $\Delta v$ . This is due to the fact that line opacity and spectral dilution effects have inverse dependency on  $\Delta v$  for optically thin ( $\tau$  below 1) lines.

The fact that the rotation temperature is low does not mean that the kinetic temperature is also low. While in the case of CO the inferred densities are high enough to make  $T_{\text{rot}} \simeq T_{\text{kin}}$ , the same is not true for  $\text{H}_2\text{O}$ . In order to determine what fraction of the absorbing  $\text{H}_2\text{O}$  belongs to which temperature component, we used the LWS-FP spectrum of the  $1_{01}-2_{12}$  pure rotational line of o- $\text{H}_2\text{O}$  (in the  $\nu_2 = 0$  level) towards Sgr A\* (see Figure 3b). It indicates that the absorption arises from three different unresolved velocity components at  $-20$ ,  $5$  and  $55 \text{ km s}^{-1}$ . The  $1_{10}-2_{21}$  line, on the other hand, only shows significant absorption at  $55 \text{ km s}^{-1}$ . This cloud is probably the one associated to Sgr A itself and as for Sgr B2 (Cernicharo et al., 1997) the analysis of the water vapor data is much more difficult due to the role of dust emission/absorption in the excitation of this molecule. Taking into account the absolute velocity accuracy of the LWS-FP, the  $-20$  and  $5 \text{ km s}^{-1}$  features could correspond to the cold  $\text{NH}_3$  (Serabyn and Güsten 1986) and CO J=3-2 (see Figure 3a). The CO absorption at  $-50 \text{ km s}^{-1}$  is marginal in the LWS-FP data of  $\text{H}_2\text{O}$ . For the physical conditions of the cold gas, a minimum opacity of  $\simeq 2$  with  $\Delta v = 12 \text{ km s}^{-1}$  is needed to produce the observed absorption. It corresponds to  $N(\text{H}_2\text{O}) > 2 \cdot 10^{14} \text{ cm}^{-2}$ . However, with this column density the contribution of the cold  $\text{H}_2\text{O}$  to the ro-vibrational absorption (SWS) will be negligible. Can we derive more precisely this column density? An answer can come from the different opacities of the pure rotational and ro-vibrational lines of  $\text{H}_2\text{O}$ .

The line profiles of the water transitions differ remarkably from those of the CO lines observed with the CSO telescope (see Figure 3a) and also with the LWS-FP instrument (data not presented here). The warm gas in Sgr A West could also produce a broad  $\text{H}_2\text{O}$  absorption, and such absorption would appear as a baseline effect in the reduced velocity coverage of the LWS-FP spectra. Such a baseline has been removed from our data but it is not possible to infer the possible contribution of the warm gas from these data. The grating data (see inset in Figure 3b), however, show an absorption feature 13% deep at the wavelength of the  $1_{01}-2_{12}$  line (and very weak absorption is also found for the  $1_{10}-2_{21}$  line), which would require  $4\times$  the absorption produced by the narrow lines of Figure 3b. Therefore, most of the absorption found in the grating spectrum must correspond to a broad velocity component badly detected with the LWS/FP. This broad absorption is also found in the 20 positions observed with the LWS grating spectrometer around Sgr A\*.

The grating data suggest a line opacity  $\simeq 1$  for a linewidth of  $200 \text{ km s}^{-1}$ . From the physical conditions we have derived for the warm gas, the  $1_{01}-2_{12}$  line opacity will be  $\sim 1$  if  $N(\text{H}_2\text{O}) = 10^{15} \text{ cm}^{-2}$ . Hence, the  $\text{H}_2\text{O}$  abundance in the warm gas is  $10^{-6}$ , similar to that found in the warm foreground gas of Sgr B2 (Cernicharo et al. 1997a, Neufeld et al. 2000). However, this column density that explains well the absorption excess in the LWS grating data is insufficient to explain the SWS absorption. Hence,

TABLE 1

Model results (T in K, N in cm <sup>-2</sup> )		
Quantity	Sgr A*	GCS-3
<b>warm gas</b>		
T <sub>K</sub> (CO & H <sub>2</sub> O)	250	
T <sub>rot</sub> (CO)	≈150	
N( <sup>12</sup> CO)	1.0 10 <sup>17</sup>	
N(H <sub>2</sub> O)	1.0 10 <sup>15</sup>	
<b>cold gas</b>		
T <sub>rot</sub> (CO)	6–12	5–10
T <sub>rot</sub> (H <sub>2</sub> O)	8	
N( <sup>12</sup> CO)	6.6 10 <sup>18</sup>	4.2 10 <sup>18</sup>
N( <sup>13</sup> CO)	1.1 10 <sup>17</sup>	0.7 10 <sup>17</sup>
N(C <sup>18</sup> O)	1.3 10 <sup>16</sup>	1.7 10 <sup>16</sup>
N(H <sub>2</sub> O)	1.9 10 <sup>16</sup>	1.2 10 <sup>16</sup>

we have to assume that the cold gas must have a larger column density to account for the SWS data.

Removing the contribution from the warm gas, the total column density of cold H<sub>2</sub>O must be 1.9 10<sup>16</sup> cm<sup>-2</sup> (three velocity components). The opacity and excitation temperature of the 1<sub>01</sub>–2<sub>12</sub> rotational line will be ≈ 90 and 7 K, respectively, for each one of the three velocity components assumed in our models. For GCS-3 we obtain a cold H<sub>2</sub>O column density of ≈ 1.2 10<sup>16</sup> cm<sup>-2</sup>. These results suggest that the lines of sight intersect dense dark clouds where most of the absorption is produced. The <sup>13</sup>CO/H<sub>2</sub>O abundance ratio would be ≈ 5.8 in both cases, i.e., <sup>12</sup>CO/H<sub>2</sub>O ≈ 350. Hence, x(H<sub>2</sub>O) ≈ 3 10<sup>-7</sup> and the water vapor gas/solid ratio is ~ 0.02 in the quiescent regions of dark clouds along the line of sight to the Galactic Center.

The water vapor abundance in the dark clouds intersecting the line of sight of Sgr A\* is much lower than that in the core of Sgr B2 and the shocked regions of Orion (see introduction). However, the total gas+ice CO/H<sub>2</sub>O abundance ratio is ≈ 5. This result means that a large fraction of the H<sub>2</sub>O molecules is condensed on grains in these cold, quiescent regions but also that the chemical mechanisms leading to its formation (either in gas phase or in the grain surface) are very efficient and make H<sub>2</sub>O the most abundant molecular species after CO.

The ISO data corresponding to the pure rotational lines of H<sub>2</sub>O towards Sgr A\* alone provide a lower limit for the

water abundance of ~ 10<sup>-8</sup>. However, when combining these data with the ro-vibrational H<sub>2</sub>O lines also observed by ISO a larger abundance, ≈ 10<sup>-7</sup>, is found. With this abundance, the pure 2<sub>12</sub>–1<sub>01</sub> and 1<sub>10</sub>–1<sub>01</sub> rotational lines of H<sub>2</sub>O in the ground vibrational state will be extremely optically thick (see above), but the expected emission from these lines will remain very low. The upper limit to the water abundance derived through emission measurements by SWAS in the direction of TMC1 (7 10<sup>-8</sup>, Snell et al. 2000) is only of factor of 4 lower than the value we derive in the dark clouds towards Sgr A\*. If we consider that in dark clouds important scattering effects have to be taken into account in the radiative transfer of optically thick lines (see Cernicharo and Guélin, 1987), the upper limit derived by SWAS could be slightly underestimated. Therefore, our results for Galactic dark clouds towards Sgr A\* and SWAS results for TMC1 would be in a relatively good agreement. Finally, absorption measurements towards continuum background sources at 556.9 GHz (1<sub>01</sub>–1<sub>10</sub>), and at 179.526 and 269.273 μm (1<sub>01</sub>–2<sub>12</sub> and 0<sub>00</sub>–1<sub>11</sub>) with future satellite missions such as FIRST, will provide a very efficient way to derive the water vapor abundance in dark clouds and in the diffuse interstellar medium.

We thank Spanish DGES for this research under grants PB96-0883 and ESP98-1351E. We thank E. González-Alfonso for useful comments. The CSO is supported by American NSF grant number AST-9980846.

## REFERENCES

- Clegg P.E., et al., 1996, A&A, 315, L38  
 Cernicharo J., Guélin M., 1987, A.&A., 176, 299  
 Cernicharo J., Thum C., Hein H., et al., 1990, A.&A., 231, L15  
 Cernicharo J., González-Alfonso E., Alcolea J., et al., 1994, ApJ, 432, L59  
 Cernicharo, J., Lim, T., Cox, et al., 1997a, A&A, 323, L25  
 Cernicharo, J., González-Alfonso, E., Lefloch, B., 1997b, in "First Workshop on Analytical Spectroscopy", 6-8 October 1997a. ESA SP-419, page 23  
 Cernicharo, J. et al. 1999, in the ESA Symposium on "The Universe as seen by ISO", P. Cox and M. Kessler, eds., ESA-SP 427, p. 565  
 Chiar, J.E., Geriakines, P.A., Whittet, D.C.B., Pendelton, Y.J., Tielens, A.G.G.M., Adamson, A.J., and Boogert, A.C.A., 2000, ApJ, 498, 716  
 Chiar, J.E., Tielens, A.G.G.M., Whittet, D.C.B., Shutte, W.A., Boogert, A.C.A., Lutz, D., van Dishoeck, E.F., Bernstein, M.P., 2000, ApJ, 537, 749  
 de Graauw, T., 1999, in "The Universe as seen by ISO", P. Cox and M. Kessler, eds., ESA-SP427, p. 31  
 Geballe, T.R., Baas, F., and Wade, R., 1989, A&A, 208, 255  
 González-Alfonso, E., Cernicharo, J., van Dishoeck, E.F., et al., 1998, ApJ, 502, L169  
 Harwit, M., Neufeld, D.A., Melnick, G.J., Kaufman, M.J. 1998, ApJ, 497, L105  
 Kessler, M.F., 1999, in "The Universe as seen by ISO", P. Cox and M. Kessler, eds., ESA-SP427, p. 23  
 Langer, W.D., and Wilson, A.A., 1990, ApJ, 357, 277  
 Lutz, D., Feuchtgruber, H., Genzel, R., et al., 1996, A&A, 315, L269

McFadzean, A.D., Whittet, D.C.B., Longmore, A.J., Bode, M.F., and Adamson, A.J. 1989, MNRAS, 241, 873  
 Moneti, A., Blommaert, J.A.D.L., Najarro, F., et al., 1999, in "The Universe as seen by ISO", P. Cox and M. Kessler, eds., ESA-SP427, p. 723  
 Neufeld et al., 2000, ApJ, 539/2, L111-113.  
 Okuda, H., Shibai, H., Nagakawa, T., Matsuhara, H., Kobayashi, Y., Nagata, T., Gatley, I., and Geballe, T.R. 1990, ApJ, 351, 89.  
 Rothman, L.S., Gamache, R.R., Tipping, R.H., et al., 1993, J. Quant. Spectrosc. Radiat. Transfer, 48, 469.  
 Schinke, R., Engel V., Buck U., et al., ApJ, 299, 939

Serabyn, E., and Güsten, R., 1986, A&A, 161, 334  
 Serabyn, E., and Güsten, R., 1991, A&A, 242, 376  
 Snell, R. L., Howe, J. E., Ashby, M. L. N., et al. 2000, ApJ, 539/2, L101-105.  
 Sutton, E.C., Danchi, W.C., Jaminet, P.A., and Masson, C.R., 1990, ApJ, 348, 503  
 van Dishoeck, E.F., Wright, C.M., Cernicharo, J., et al., 1998, ApJ, 502, L173  
 Whittet, D.C.B., Boogert, A.C.A., Geriakines, P.A., Schutte, W.A., Tielens, A.G.G.M., de Graauw, T., Prusti, T., van Dishoeck, E.F., Wasselius, P.R., and Wright, C.M., 1997, ApJ, 490, 729

FIG. 1.— ISO/SWS spectra of the stretching mode of CO (a,b,c) and the bending mode of water vapor (d,e,f) in the direction of Sgr A\* (ISO observation number, ION, 46301102). Panels (a) and (d) show the observations and the adopted continuum (including ices); panels (b) and e show the contribution of the ices and of the warm CO; panels (c) and (f) show the normalized spectrum and model spectrum (shifted for clarity), and panel (g) shows the details of the ortho- and para-H<sub>2</sub>O transitions.

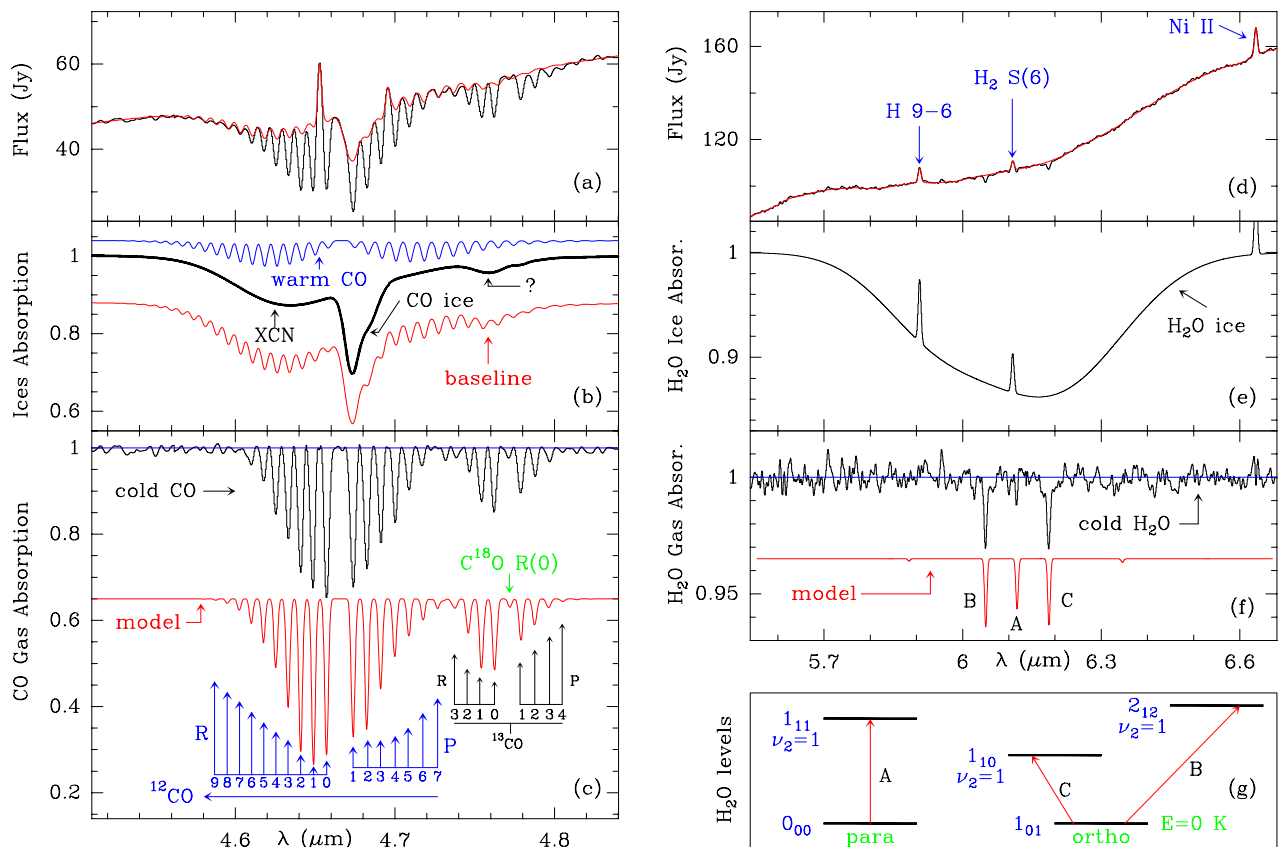


FIG. 2.— CO spectrum and model for GCS-3 (ION 32701543). Panel (a) shows the observations and the adopted continuum (including ices); panel (b) shows the contribution of the ices and of the warm CO; panel (c) shows the normalized spectrum and model spectrum (shifted for clarity)

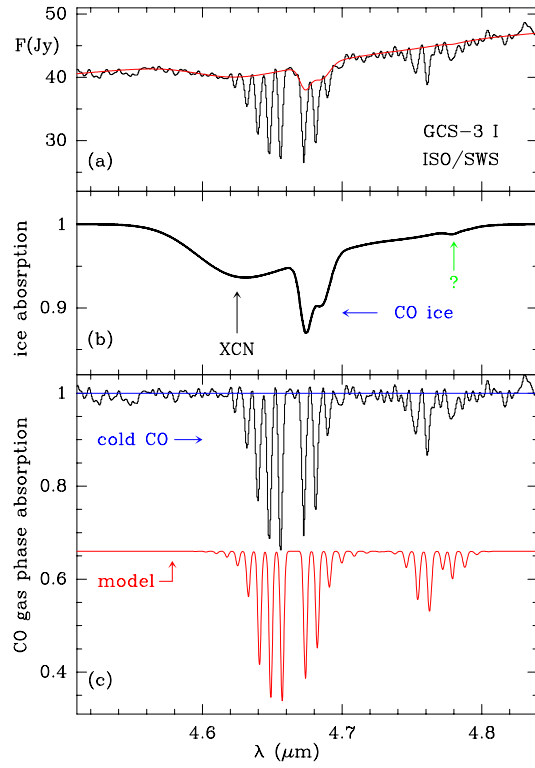


FIG. 3.— (a) J=3-2 and J=7-6 lines of CO observed at the CSO towards Sgr A\*. The downwards arrows indicate the central position of the cold gas absorption features. The upwards arrows indicates the velocity of the Sgr A West molecular cloud. (b) LWS-FP spectra of the  $2_{12}$ - $1_{01}$  and  $2_{21}$ - $1_{10}$  lines of o-H<sub>2</sub>O toward Sgr A\* (IONs 46300809 & 46900837). The drawing at bottom left indicates the transitions levels involved. The  $1_{01}$ - $2_{12}$  line shows three unresolved components at  $v = 20, 5$  and  $55 \text{ km s}^{-1}$  while in the other transition only the  $55 \text{ km s}^{-1}$  feature is present. The uncertainty in the absolute velocity  $\simeq 10\text{--}15 \text{ km s}^{-1}$ . The inset panel shows the LWS-grating spectrum (IONs 28701825, 32600211, 32702049, 49801004, 50501346, 67701010, 85302208 & 82800298); the CO and H<sub>2</sub>O lines are indicated. The LWS-FP spectrum of o-H<sub>2</sub>O has been shifted in velocity by 1/3 of the spectral resolution in order to match the velocity of the absorption features of other molecular species including CO. The upwards arrows indicate the velocities of the cold absorbing gas and the downwards arrow that of the Sgr A\* molecular cloud.

